An Artificial Neural Network approach to Laser-Induced Breakdown Spectroscopy Quantitative Analysis

Eleonora D'Andrea[a], Stefano Pagnotta[b], Emanuela Grifoni[b], Giulia Lorenzetti[b], Stefano Legnaioli[b], Vincenzo Palleschi[b], Beatrice Lazzerini[a]

[a] Department of Information Engineering, Largo Lucio Lazzarino 1, 56122 Pisa (ITALY)

[b] Applied Laser Spectroscopy Laboratory, Institute of Chemistry of Organometallic Compounds, Research Area of CNR, Via G. Moruzzi 1, 56124 Pisa (ITALY)

Abstract

The usual approach to Laser-Induced Breakdown Spectroscopy (LIBS) quantitative analysis is based on the use of calibration curves, suitably built using appropriate reference standards. More recently, statistical methods relying on the principles of Artificial Neural Networks (ANN) are increasingly used. However, ANN analysis is often used as a 'black box' system and the peculiarities of the LIBS spectra are not exploited fully. An *a priori* exploration of the raw data contained in the LIBS spectra, carried out by a Neural Network to learn what are the significant areas of the spectrum to be used for a subsequent Neural Network delegated to the calibration, is able to throw light upon important information initially unknown, although already contained within the spectrum. This communication will demonstrate that an approach based on neural networks specially taylored for dealing with LIBS spectra would provide a viable, fast and robust method for LIBS quantitative analysis. This would allow the use of a relatively limited number of reference samples for the training of the network, with respect to the current approaches, and provide a fully automatizable approach for the analysis of a large number of samples.

KEYWORDS: Laser-Induced Breakdown Spectroscopy, Artificial Neural Networks, Quantitative Analysis, Bronze

Correspondig author: Vincenzo Palleschi, e-mail: vincenzo.palleschi@cnr.it

1. Introduction

The feasibility of Laser-Induced Breakdown Spectroscopy (LIBS) as an analytical technique has been demonstrated by a number of applications on solid, liquid and gas samples [1- 3]. However, the wide literature accumulated in the last years has also demonstrated the main problems related to LIBS analysis, i.e. its limited sensitivity and, most of all, the poor precision of the technique, which also affects the global accuracy of the results [4].

In the attempt of improving this figure of merit, several groups have proposed the use of statistical methods for the treatment of the LIBS spectra, such as Partial Least Squares (PLS) [5-7] or Artificial Neural Networks (ANN) approaches [8-10]. The application of statistical algorithms has the advantage of exploiting very well the intrinsic speed of the LIBS technique, which makes possible the acquisition of many spectra in a very short time. The negative side of these algorithms is related to the need of a careful validation of the results obtained; in fact, as in all the methods based on calibration curves or reference samples, the capability of the statistical algorithm to reproduce well the composition of the calibration set does not automatically imply that the composition of unknown samples would be predicted with the same trueness [11]. In the case of Artificial Neural Networks, the validation of the method is made even more difficult by the fact that the complexity of the algorithm does not allow an easy interpretation of the results in terms of the physical properties of the system under study. Moreover, the wide availability of ANN packages in the most diffused statistical software (Matlab®, Statistica®, etc…) allows their use even by persons without any specific knowledge of the potential, but also of the limits, of these approaches. This contributes to the naïve idea of the Artificial Neural Network as a king of thinking 'organism' doted by an artificial intelligence that would provide in any case optimal results, without need for any external human intervention. In fact, taking literally the analogy, an ANN would be a very poor representation of the thinking mechanism of the human brain; the elemental operator in a Neural Network, the 'neuron', has in common with its natural equivalent just the capability of accepting multiple 'inputs' and providing an eventually non-linear response signal depending on them. Moreover, in the common implementation of an ANN, the algorithm exploits a very simple topology of the network, were the processing of the information proceeds along a given direction, from the input to the output through a series of 'layers' in which the neurons take the input from the previous and give their output to the next, without any interaction between the neurons of the same layer. The 'learning' stage of this kind of ANN is thus nothing else that the iterative optimization on a set of reference samples of the parameters of each neuron for obtaining, starting from a given input, an output as close as possible to the known results. On the other hand, this stage is essential for improving the predictive potential of an ANN and should be carefully planned because the training of the Network, as well as the choice of its architecture, very seldom can be optimized using the default values proposed by the commercial statistical packages.

2. Experiment

In this paper we present a methodological approach for dealing with the problem of modeling the functional relationship between LIBS spectra and the corresponding composition of a set of samples, using ANN. For this study, we used six different samples of modern bronze alloys with known

concentrations, previously measured by X-Ray Fluorescence, of four elements: Cu, Zn, Sn, and Pb. The composition (percent in weight) of the samples is shown in Table 1.

Table 1. Composition of six samples of modern bronze alloys.

Sample Id	Composition			
	Copper (%)	**Zinc (%)**	**Tin (%)**	**Lead (%)**
S160	83.6	1.9	11.4	3.1
S161	87.1	5	5.5	2.4
S162	90.9	0.3	7.8	1
S163	84.1	1.4	10.5	4
S164	85.7	9.5	3.6	1.2
S165	87.3	3.7	6.6	2.4

The same samples were used in a recent work by our group, presenting a variation of the Calibration-Free LIBS method [12]. In this way, the results of the present paper would be immediately comparable with a different analytical approach which in principle does not rely on the use of calibration curves or reference samples.

The LIBS measurements on the bronze samples were performed using the Modì (Mobile Dual Pulse Instruments) by Marwan s.r.l. (Pisa, Italy) in the 'Smart' configuration [13]. The instrument is equipped with a double pulse Q-switched Nd-YAG laser (λ= 1064 nm), giving two collinear pulses with an energy of 60 mJ per pulse in about 8 ns, at a repetition rate of 10 Hz.

The analysis was performed inside the internal experimental chamber of the instrument. The sample was set in rotation for reducing the depth of the laser-induced crater. The delay between the two lasers was fixed to 1 μs and the acquisition delay of the spectrometer was set to 260 ns after the second laser pulse. The two laser beams were focused on the sample surface using a 10 cm focal length lens. The plasma radiation was collected using an optical fiber and analyzed with a double grating spectrometer (AvaSpec Dual-Channel Fiber Optic Spectrometer from Avantes), covering simultaneously the spectral interval between 200 and 415 nm (with resolution of 0.1 nm) and between 415 and 900 nm (with resolution of 0.3 nm). For each of the six samples 150 single spectra were acquired, distributed on a circular portion of the sample determined by its rotation. A total of 900 single spectra were acquired and processed.

A typical spectrum is shown in Figure 1.

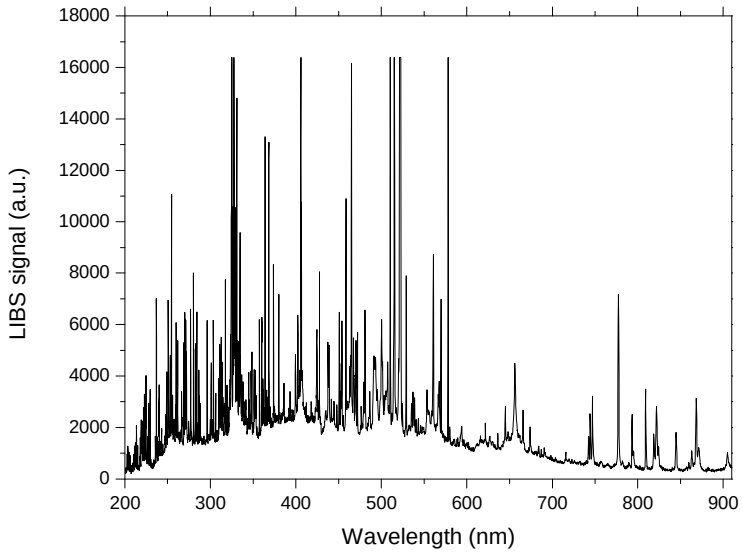

Fig. 1. LIBS spectrum of one of the bronze alloys (sample S160).

3. The approximating neural model

3.1. Problem description

The LIBS spectra of the samples represent the intensity of the LIBS signal (expressed as an integer between 0 and 16383, 14 bits) at 3606 wavelengths. This means that the problem of associating each spectrum with the corresponding composition might be described as the approximation of a functional relationship between an input in $\Im^{3606}$ and an output in $\Re^4$ (representing the concentrations of the four main elements in the alloy), based on a set of data (900 in our case). The strategy of using all the spectral data as the input of the Neural Network has been used, in the past, but this approach is not appropriate, for its high computational cost and the likelihood of function overfitting [14]. The output of a functional relationship must thus be determined by a subset of the input variables. One theoretical possibility would be to exhaustively evaluate all possible combinations of the input variables (typically referred to as *features*), and then choose the best subset. Of course, the implied computational cost could be prohibitive, as in our case. For this reason, other methods have been proposed.

One of the most frequently used methods for variable selection is the *forward feature selection* (FFS) [15], which begins by evaluating all feature subsets consisting of only one feature. Then FFS finds the best subset consisting of two features (the one previously selected and another feature from the remaining ones). Afterwards, FFS finds the best subsets with three, four, etc. features. The final best subset is the best among all the subsets generated. Of course, when the number of features that undergo feature selection is sensibly high (e.g., of the order of a few thousands), FFS too may be too expensive.
Taking into account the above observations, in this paper, we have adopted a hybrid approach in order to find a good trade-off between high accuracy and small size of the approximating model. More precisely, based on heuristic considerations, we first identify a set of portions of the LIBS spectrum in which we

expect to find information useful to model the input-output relationship. We will refer to the identified portions as *meaningful* spectral windows of the LIBS spectrum. Then we perform FFS on the union of these spectrum windows. In this way we make an effective use of FFS by keeping time and computational costs at acceptable levels.

3.2. Methodology steps

The proposed methodology includes two main steps: i) feature selection on the union of the meaningful spectral windows of the LIBS spectrum, and ii) development of a neural network whose input variables are the selected features. The second step includes training, checking and testing of the network.

3.2.1. Feature selection

Hereafter, each spectral line will be referred to as feature. The feature selection step aims to find the most significant features able to discriminate among the different bronze alloys. Stated in other terms, we want to transform the input space, i.e., $\Im^{3606}$, into a space $\Im^{n}$ with $n << 3606$, by guaranteeing at the same time the possibility to reproduce the mapping between spectra and alloys' compositions with the desired accuracy. The intensities of the selected spectral lines will be the input variables of a neural network trained to faithfully reproduce the mapping itself.

To reduce the dimensionality of the problem, we perform a preliminary step. Based on heuristic considerations, we consider the following six meaningful spectral windows (wavelength ranges in nanometers) [279.7-286.6], [295.8-306.6], [324.5-335.0], [356.9-369.5], [405.0-407.0], [640.0-680.0], corresponding to intervals including wavelengths already successfully used for a Calibration-Free measurement of the composition of the bronze alloys under analysis [12]. This means that there are 480 spectral points (obtained by concatenating the six spectral windows above) that could be used to represent each spectrum. So each spectrum could be represented in $\Im^{480}$. These features are still too many. In fact, heuristic guidelines state that there should be from five to ten training examples for each neural weight.
Therefore we perform a feature selection process using the FFS [16]. As previously stated, FFS consists in iteratively picking the feature that, in union with the features selected so far, optimizes the quality function. In our case, the quality function is the error made by the neural network on the test set.
More precisely, for each set of features generated by FFS, a neural network with these features as input variables is considered. Let n be the number of features in the set. The network has n input neurons, 10 hidden neurons (for the sake of simplicity, in this phase of the modeling process, we have maintained the default value proposed by Matlab®) and 4 output neurons. This network is trained, validated and tested with 70%, 15% and 15%, respectively, of the 900 available spectra. Here too we maintain the default values proposed by Matlab®. The network is evaluated based on the mean square error (MSE) made on the test set.
As the error of the network may depend on the initial random values of the neural weights, for each network the experiment is repeated 30 times and the error of the network is actually computed as the average of MSEs over the 30 executions.
For improved efficiency and reliability, we repeat the whole FFS process more times so as to select "stable" features, i.e., features that appear in all (or most of) the experiments. Indeed, the features selected by the FFS may vary from one trial to another. In order to guarantee a higher level of generalization, we are, therefore, interested in identifying the minimum number of features that are significant for all (or

most of) the training sets. We set the number of repetitions of the FFS to 30, which is suggested by [16] to be a typical value used in simulation. At the same time, in each trial we fix a maximum number of features equal to 10 (based on heuristic considerations) so as to keep the computational complexity at an acceptable level.

3.2.2. Neural network development

The most used Neural Network architecture and training algorithm are the multi-layer feed-forward neural network (MLP), and the Levenberg-Marquardt (LM) *back-propagation* training algorithm [17], which shows good generalization capability and simplicity.
In an MLP there are three kinds of layers: i) the *input layer* which receives the input signals, ii) one or more *hidden layers* where the processing takes place, and iii) the *output layer* which provides the output. Neurons in each layer are characterized by a specific transfer function. In particular, hidden neurons usually have a non-linear transfer function, while output neurons may have a linear or non-linear transfer function. The number of hidden neurons is chosen experimentally to minimize the average error across all training patterns.
In this step, we refer to an MLP neural network with fixed numbers of input and output neurons, and a single hidden layer with a variable number of neurons. More precisely, the stable features identified in the previous step are used as input variables of the network, while the concentrations of the four elements represent the output variables of the network. As far as the hidden layer is concerned, based on best practices and considering the available data, we try a number of hidden neurons from 5 to 20 with step 1. For each number of hidden neurons, the network is trained 10 times. In each of the 10 trials, we generate different training, validation and test sets (70%, 15% and 15%, respectively, of the total data). The final best network is the one corresponding to the minimum average MSE on the 10 different testing sets.

3.3. Analysis

3.3.1. Data preprocessing

As a preprocessing phase, the input features are normalized in [0, 1] in order to make the features independent from each other. To this aim, we rescale each input value according to the max-min formula in Eq. (1):

$$x' = \frac{x - \min(x)}{\max(x) - \min(x)}, \quad (1)$$

where x is the original value, x' is the normalized value, and $max(x)$ and $min(x)$ are the maximum and minimum values that x can take, respectively.

3.3.2. Feature selection

The FFS process applied to the 480 features was repeated 30 times. We noticed that, after adding the 4-th feature, in almost all the executions of the FFS process the MSE error deeply increases while in the rest of the executions the error does not decrease in a meaningful way. So we decided to consider only three input features for the problem.

The most frequent set of three SFs throughout all the executions of the FFS process resulted to be the set of LIBS intensities corresponding to the wavelengths (in nanometers) {334.45, 329.05, 304.81}. The feature corresponding to the wavelength 334.45 nm, associated to a strong emission line of Zn I, always resulted to be the most discriminant feature, being selected as the first one in all repetitions of the FFS process. In fact, if we plot all the 900 spectra from the six bronze samples, we can easily see how the six samples are clearly separated and distinguishable in correspondence of wavelength 334.45 nm, while they are almost completely overlapping in correspondence of the neighboring spectral lines (Fig. 2). The second wavelength corresponds to the emission line of a Cu I line (329.05 nm), while the third wavelength is not associated to any spectral line. Note that three independent spectral features are the minimum number needed for determining the concentration of the four major elements of the bronze alloys, since the closure condition of the total composition to 100% imposes a further relation to be fulfilled, allowing in principle the determination of the four elements considered.

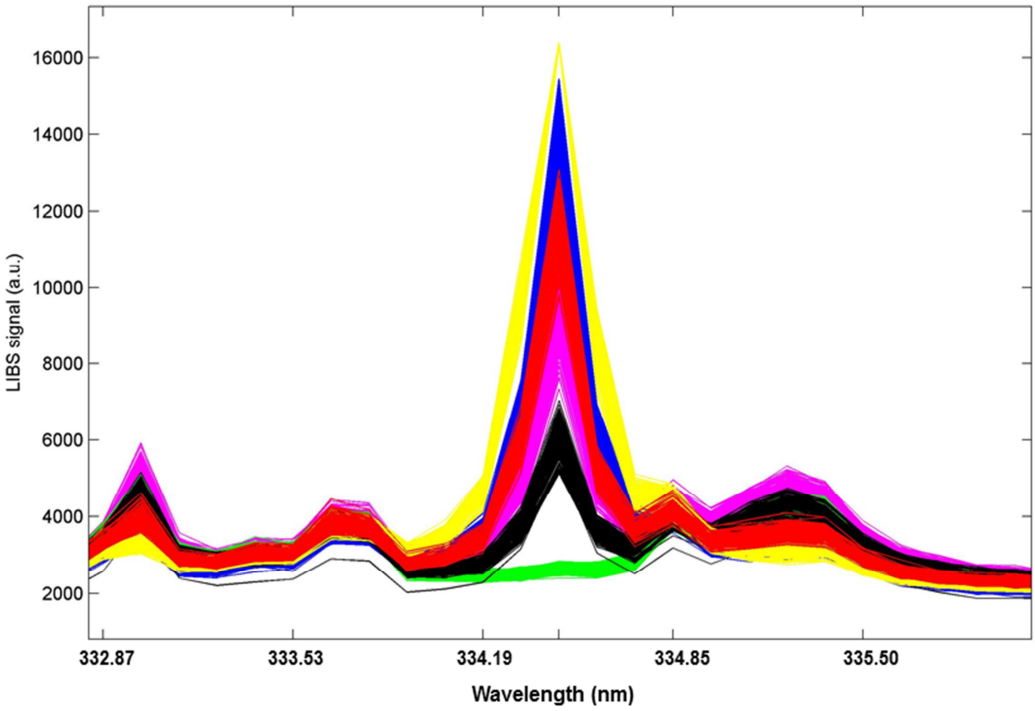

Fig. 2. The 900 spectra of the six bronze samples in correspondence of wavelength 334.45 nm. Each color corresponds to the spectra of a sample.

3.3.3. Neural network development

We adopted the set of features {334.45, 329.05, 304.81} to develop the neural network model. We used a feed-forward neural network with one hidden layer, to implement the fitting model. The neural network had three inputs (the spectral lines selected) and four outputs (the element concentrations to be associated to the inputs). The transfer functions for the hidden neurons and the output neurons are, respectively, hyperbolic tangent sigmoid function and linear functions, as Fig. 3 shows.

In order to find the optimal number of hidden neurons, we tried a number of hidden neurons from 5 to 20 with step 1, as stated before. The optimal number of hidden neurons resulted to be 15. Table 2 summarizes the parameter values of the chosen neural configuration.

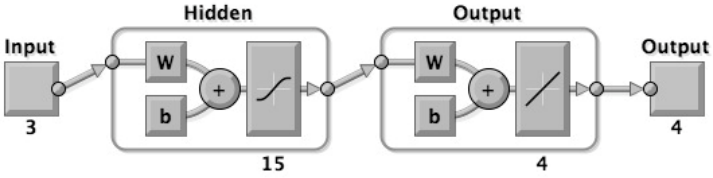

Fig. 3. Network model employed in the experiments. The model has 3 inputs, 15 hidden neurons with hyperbolic tangent sigmoid transfer function, and 4 outputs with linear transfer function (the figure was depicted in the Matlab® environment).

Table 2. Parameters of the neural network model employed.

Parameter	Value
Number of hidden layers	1
Number of hidden neurons	15
Transfer functions	Hyperbolic tangent sigmoid (hidden layer), linear (output layer)
Training algorithm	Levenberg-Marquardt
Early stopping criterion	6 validation failures
Number of input variables	3
Number of output variables	4

3.3.4. Fitting the composition of known samples

By "known" sample we mean a sample shown to the neural network during the training process. This first kind of experiment aims to estimate the performances of the Neural Network on the reference samples, given the SFs and the number of hidden neurons previously established. In particular, we include examples (spectra) from all the six samples of bronze alloys into the training set, and test the network on spectra, again from each sample, but unseen during training.

We repeated the training and test of the neural network 30 times, each time exploiting different, randomly generated, training, test and validation sets corresponding to, respectively, 70%, 20%, and 10% of the totality of data. These percentages have been chosen to exploit the available data for testing purposes as better as possible.

For each trial, to evaluate the goodness of the network, we used the Mean Square Error (MSE) on the test set defined in Eq. (2):

$$MSE = \frac{1}{S}\sum_{i=1}^{S}(t_i - o_i)^2 , \qquad (2)$$

where t_i and o_i are, respectively, the *target* and *estimated* concentration values associated with spectrum *i*, and *S* is the number of test spectra considered.

We achieved a mean MSE on the 30 test sets of $2.793 \cdot 10^{-3}$ with a standard deviation of $5.292 \cdot 10^{-3}$.

For a better interpretation of the results, we also considered the Mean Absolute Error (MAE), defined in Eq. (3):

$$MAE = \frac{1}{S}\sum_{i=1}^{S}\left|t_i - o_i\right|. \tag{3}$$

We achieved a mean MAE on the 30 test sets of $9.090 \cdot 10^{-3}$ with a standard deviation of $1.116 \cdot 10^{-2}$.

To assess the goodness of the model, we used two further tools, namely, the regression graph and the error histogram.

With reference to one of the 30 executions of the experiment, Fig. 5 shows the regression graph for the training, validation, and test sets, and the whole data set: the R value = 1 indicates an optimal linear fitting of the model to the data; Fig. 6 shows the error histogram for the training, validation and test sets: almost all training, validation and test examples have errors significantly close to zero. All the other executions of the experiment produce similar results.

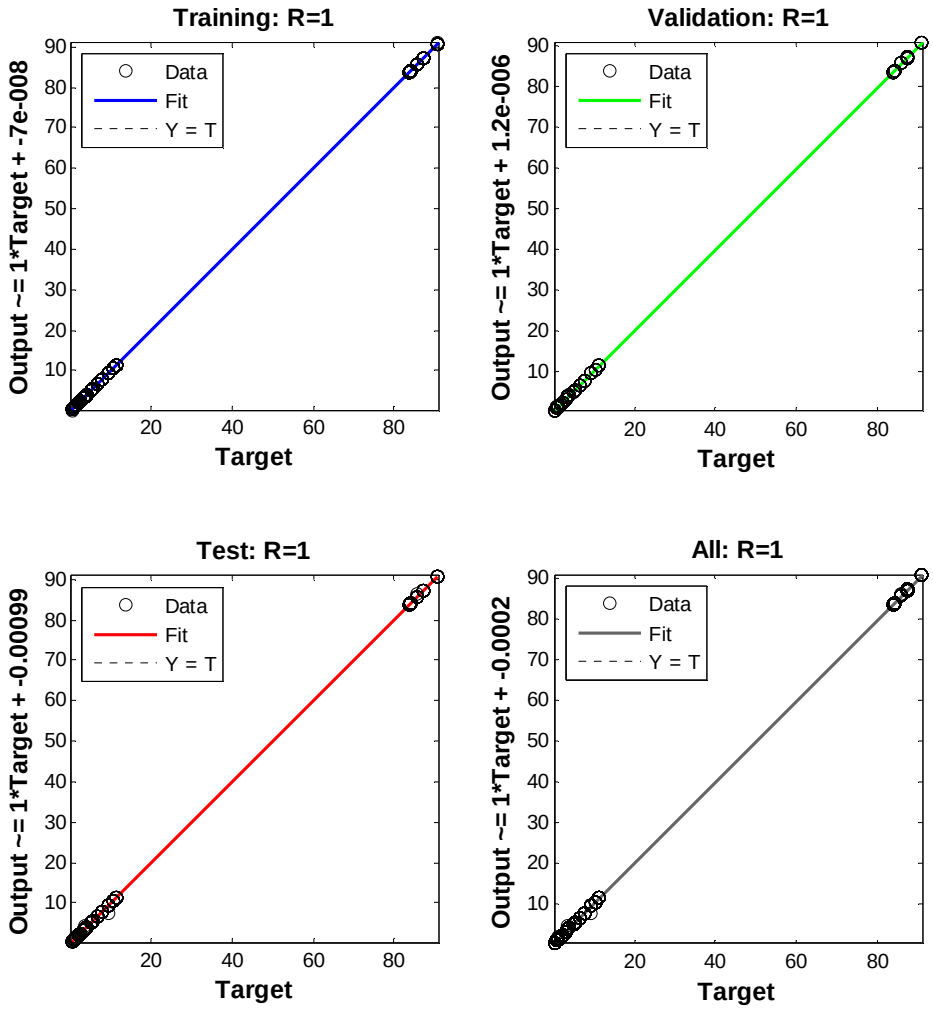

Fig. 4. The regression graph.

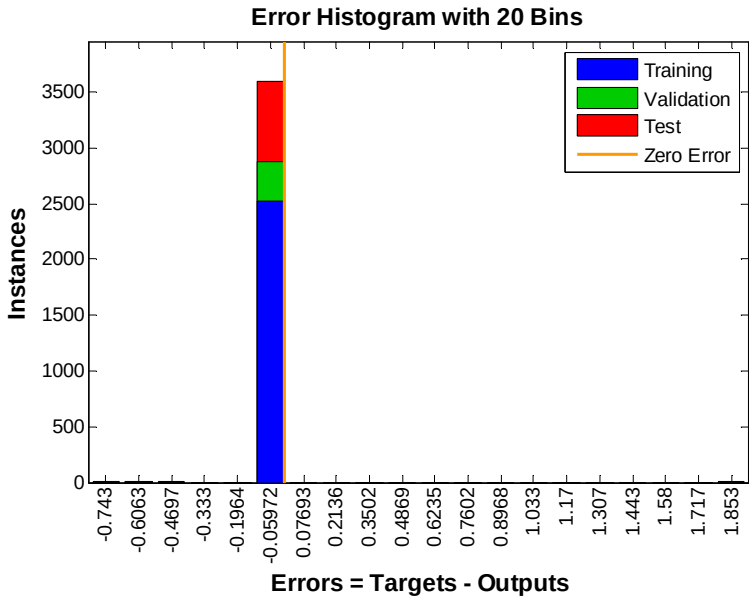

Fig. 5. The error histogram.

To assess the validity of the model, we also computed the test error (MSE and MAE) achieved on the spectra of each sample separately, and the test error (MSE and MAE) achieved on each element separately (independently of the sample), over the 30 trials. Table 3 shows the mean MSE and mean MAE obtained over the 30 executions by sample. Table 4 shows the mean MSE and mean MAE obtained over the 30 executions by element.

Table 3. Mean MSE and mean MAE by sample.

Sample Id	MSE	MAE
S160	$1.208 \cdot 10^{-3}$	$1.024 \cdot 10^{-2}$
S161	$5.483 \cdot 10^{-4}$	$7.939 \cdot 10^{-3}$
S162	$2.409 \cdot 10^{-4}$	$5.191 \cdot 10^{-3}$
S163	$2.039 \cdot 10^{-3}$	$1.475 \cdot 10^{-2}$
S164	$1.441 \cdot 10^{-2}$	$1.228 \cdot 10^{-2}$
S165	$2.720 \cdot 10^{-4}$	$6.838 \cdot 10^{-3}$

Table 4. Mean MSE and mean MAE by element.

Element	MSE	MAE
Copper	$1.123 \cdot 10^{-3}$	$7.436 \cdot 10^{-3}$
Zinc	$6.853 \cdot 10^{-3}$	$1.091 \cdot 10^{-2}$
Tin	$2.165 \cdot 10^{-3}$	$1.059 \cdot 10^{-2}$
Lead	$1.030 \cdot 10^{-3}$	$7.417 \cdot 10^{-3}$

3.3.5. Determining the composition of unknown samples

By “unknown” sample we mean a sample not shown to the neural network during the training process. In this second kind of experiment, we use only a subset of the six samples to train the neural network, and we test the network on the remaining samples.

The choice of the training and ‘unknown’ samples was done starting from the consideration that the ANN method, as all the methods based on reference or calibration samples, can be only used for analyzing samples whose concentrations are upper and lower limited by the minimum and maximum concentrations of the samples in the training (calibration) set [18].

For instance, referring to Table 1, we can notice that the Cu element assumes the minimum and the maximum value in correspondence with sample S160 and sample S162, respectively. Thus samples S160 and S162 are chosen as training samples. The Zn concentration has its minimum and maximum for samples S162 and S164. Since sample S162 is already in the training set, only sample S164 has to be added. The same considerations on the concentrations of lead and tin result in a complete training set corresponding to the samples {S160, S162, S163, S164}.

In the experiments, a neural network with the configuration of Fig. 3, was trained, validated, and tested on the spectra in the set of samples {S160, S162, S163, S164}, using randomly generated sets of, respectively, 90%, 5%, and 5% spectra. These percentages have been chosen to exploit the available data for training purposes as better as possible. The experiment was repeated 30 times, and each time the network (besides being tested on the 5% of the known spectra, exactly as in the previous kind of experiment) was tested also on the spectra of the unknown samples S161 and S165 separately.

We would like to stress that this is the only really discriminating test on the analytical capabilities of the Neural Network, because during the training set the samples S161 and S165 were never presented to the network, so they can be considered as truly ‘unknown’. In other words, the knowledge of their composition is exploited only for assessing the accuracy of the ANN, as shown in the regression graphs of Figure 6a and 6b. Table 5 shows the mean MSE, the mean MAE, and their standard deviation, achieved on samples S161 and S165 over the 30 trials.

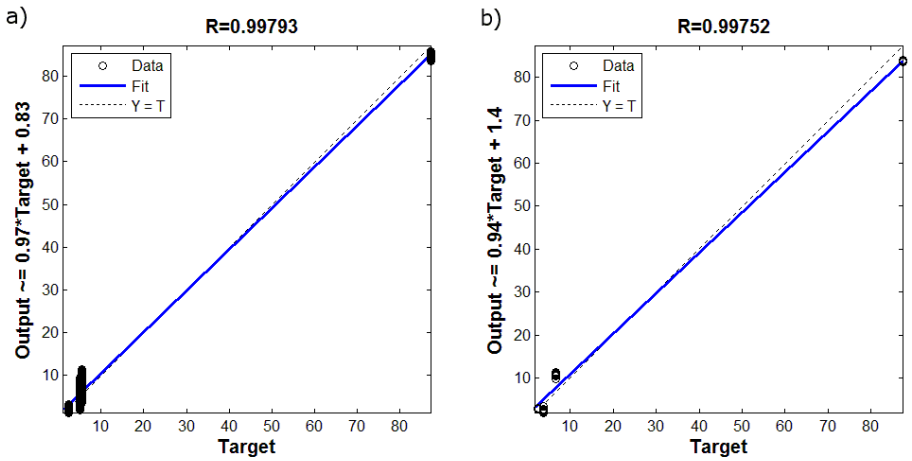

Fig. 6. Regression graph for a) Sample S161, b) Sample S165.

Tables 6 and 7 show the results (mean concentration, mean MSE and mean MAE) obtained by element on samples S161 and S165, respectively.

Table 5. Mean MSE and mean MAE on samples S161 and S165.

Sample Id	MSE	MAE
S161	5.948	2.075
S165	8.26	2.41

Table 6. Mean concentrations, mean MSE and mean MAE on sample S161 by element.

Element	Concentration	MSE	MAE
Copper	85	2.133	1.406
Zinc	6	16.486	3.958
Tin	7	3.842	1.814
Lead	2	1.333	1.123

Table 7. Mean concentrations, mean MSE and mean MAE on sample S165 by element.

Element	Concentration	MSE	MAE
Copper	84	12.535	3.534
Zinc	2	2.020	1.336
Tin	11	18.151	4.195
Lead	3.1	0.345	0.565

The ANN results can be considered quite precise (the mean average error for all the elements is around 2%), also considering the fact that only four reference samples were used for the training and only three LIBS intensities were used, out of a spectrum of 3606 elements. However, it should also be considered that the ANN algorithm used aims to the minimization of the total MSE; therefore, the relative uncertainty on the elements at higher concentration will be proportionally lower than the relative error on the elements at low concentration. For example, the copper concentration obtained for sample S165 corresponds to about 84 ± 4 % (less than 5 % relative error) while the zinc concentration corresponds to about 2 ± 1 % (50 % relative error). For obtaining a better estimation of the low concentration elements, a transformation of the target concentration (through the application of a square root or logarithmic function) would have been needed.

As a final consideration, we would like to compare the present approach with the results of the application of the One-Point Calibration CF-LIBS method reported, on the same samples, in ref. [12]. The data for sample S165 (sample S161 cannot be compared because it was used as a reference in [12]) are reported in Table 8.

Table 8. Nominal concentrations, ANN results and OPC results (ref. [12]) on sample S165 by element.

Element	Nom. concentration (%)	ANN (%)	OPC (%) [12]
Copper	87.3	84	86.6
Zinc	3.7	2	4.0
Tin	6.6	11	7.6
Lead	2.4	3.1	1.9

Apparently, the OPC CF-LIBS method gives more accurate results, although it does not make use of reference samples (besides one, for the reasons explained in the paper); however, the CF-LIBS approach requires the use of complex algorithms which are not easy to apply to the analysis of a large number of spectra, as in the present case. The Artificial Neural Network method, on the contrary, would take some time for its optimization but, after that, it will perform in a very short time the analysis of a large number of spectra in a completely automatic way.

4. Conclusion

In this paper we have presented a methodological approach to the LIBS analysis using the Artificial Neural Networks method. A preliminary step of dimension reduction has been foreseen so as to achieve the desired accuracy while keeping the complexity of the approximating neural model as low as possible. To this aim, the *forward feature selection* has been adopted to reduce the number of input variables (the intensities of the spectral lines) to the neural network to the minimum number of variables, representing the features selected as the most significant variables for approximating the functional relationship. We performed a detailed optimization of the inputs of the network so as to study the presence of matrix-specific information in the inputs examined. The adopted neural model is a multi-layer feed-forward neural network with three input neurons, one hidden layer, and four output neurons. With the aim of applying the Network for the analysis of the composition of bronze alloys, we used a significant subset of the samples to train the neural network, and we tested the network on the remaining ‘unknown’ samples. As a result of this experiment, we were able to achieve acceptable values of trueness and precision in a way that could be easily automatized, for example, for the continuous monitoring of the composition of large numbers of metal samples in industrial applications.

References

[1] Corsi, M., Cristoforetti, G., Hidalgo, M., Iriarte, D., Legnaioli, S., Palleschi, V., Salvetti, A., Tognoni, E., Temporal and spatial evolution of a laser-induced plasma from a steel target, *Appl. Spectrosc*., **57** (6) (2003) 715-721.

[2] Mbesse Kongbonga, Y.G., Ghalila, H., Onana, M.B., Ben Lakhdar, Z., Classification of vegetable oils based on their concentration of saturated fatty acids using laser induced breakdown spectroscopy (LIBS), *Food Chemistry*, **147** (2014) 327-331.

[3] D'Ulivo, A., Onor, M., Pitzalis, E., Spiniello, R., Lampugnani, L., Cristoforetti, G., Legnaioli, S., Palleschi, V., Salvetti, A., Tognoni, E., Determination of the deuterium/hydrogen ratio in gas reaction products by laser-induced breakdown spectroscopy, *Spectrochim. Acta B*, **61** (7) (2006) 797-802.

[4] Winefordner, J.D., Gornushkin, I.B., Correll, T., Gibb, E., Smith, B.W., Omenetto, N., Comparing several atomic spectrometric methods to the super stars: Special emphasis on laser induced breakdown spectrometry, LIBS, a future super star, *J. Anal. Atom. Spectrom.*, **19** (9) (2004)1061-1083.

[5] Goode, S.R., Morgan, S.L., Hoskins, R., Oxsher, A., Identifying alloys by laser-induced breakdown spectroscopy with a time-resolved high resolution echelle spectrometer, *J. Anal. Atom. Spectrom.*, **15** (9) (2000) 1133-1138.

[6] Andrade, J.M., Cristoforetti, G., Legnaioli, S., Lorenzetti, G., Palleschi, V., Shaltout, A.A., Classical univariate calibration and partial least squares for quantitative analysis of brass samples by laser-induced breakdown spectroscopy, *Spectrochim. Acta B*, **65** (8) (2010) 658-663.

[7] Wang, Z., Feng, J., Li, L., Ni, W., Li, Z., A multivariate model based on dominant factor for laser-induced breakdown spectroscopy measurements, *J. Anal. Atom. Spectrom.*, **26** (11) (2011) 2289-2299.

[8] Moros, J., Serrano, J., Gallego, F.J., Macías, J., Laserna, J.J., Recognition of explosives fingerprints on objects for courier services using machine learning methods and laser-induced breakdown spectroscopy, *Talanta*, **110** (2013) 108-117.

[9] Caceres, J.O., Moncayo, S., Rosales, J.D., De Villena, F.J.M., Alvira, F.C., Bilmes, G.M., Application of laser-induced breakdown spectroscopy (LIBS) and neural networks to olive oils analysis, *Appl. Spectrosc*., **67** (9) (2013) 1064-1072.

[10] Boueri, M., Motto-Ros, V., Lei, W.-Q., Ma, Q.-L., Zheng, L.-J., Zeng, H.-P., Yu, J., Identification of polymer materials using laser-induced breakdown spectroscopy combined with artificial neural networks, *Appl. Spectrosc.*, **65** (3) (2011) 307-314.

[11] Palleschi, V., Comment on "a multivariate model based on dominant factor for laser-induced breakdown spectroscopy measurements" by Zhe Wang, Jie Feng, Lizhi Li, Weidou Ni and Zheng Li, J. Anal. At. Spectrom., 2011, DOI: 10.1039/c1ja10041f, *J. Anal. Atom. Spectrom.*, **26** (11) (2011) 2300-2301.

[12] Cavalcanti, G.H., Teixeira, D.V., Legnaioli, S., Lorenzetti, G., Pardini, L., Palleschi, V., One-point calibration for calibration-free laser-induced breakdown spectroscopy quantitative analysis, *Spectrochim. Acta B*, **87** (2013) 51-56.

[13] Bertolini, A., Carelli, G., Francesconi, F., Francesconi, M., Marchesini, L., Marsili, P., Sorrentino, F., Cristoforetti, G., Legnaioli, S., Palleschi, V., Pardini, L., Salvetti, A., Modì: A new mobile instrument for in situ double-pulse LIBS analysis, *Anal. Bioanal. Chem.*, **385** (2) (2006) 240-247.

[14] Marcos-Martinez, D., Ayala, J.A., Izquierdo-Hornillos, R.C., De Villena, F.J.M., Caceres, J.O., Identification and discrimination of bacterial strains by laser induced breakdown spectroscopy and neural networks, *Talanta*, **84** (3) (2011) 730-737.

[15] Haykin, S.S., *Neural networks. A comprehensive foundation*, Second Edition, Prentice-Hall, New Jersey, U.S (1999).

[16] Kuncheva, L.I., *Combining pattern classifiers: Methods and algorithms*, Wiley Interscience, New Jersey, U.S. (2004).

[17] Rumelhart, D.E., Hinton, G.E., Williams, R.J., Learning representations by back-propagating errors, *Nature*, **323** (1986) 533–536.

[18] International Union of Pure and Applied Chemistry, Guidelines for calibration in analytical chemistry, Part 1. Fundamentals and single component calibration, *Pure & Appl. Chem*., **70** (4) (1998) 993-1014.